Arch. Metall. Mater. **64** (2019), 2, 773-778

DOI: 10.24425/amm.2019.127612

M. SZKLARSKA*#, B. ŁOSIEWICZ*, G. DERCZ*, M. ZUBKO*, R. ALBRECHT*, D. STRÓŻ*

CHARACTERIZATION OF LONG-TERM CORROSION PERFORMANCE OF Ti15Mo ALLOY IN SALINE SOLUTION

The Ti15Mo alloy has been studied towards long-term corrosion performance in saline solution at 37°C using electrochemical impedance spectroscopy. The physical and chemical characterization of the material were also investigated. The as-received Ti15Mo alloy exhibits a single β-phase structure. The thickness of single-layer structured oxide presented on its surface is ~4 nm. Impedance measurements revealed that the Ti15Mo alloy is characterized by spontaneous passivation in the solution containing chloride ions and formation of a double-layer structured oxide composed of a dense interlayer being the barrier layer against corrosion and porous outer layer. The thickness of this oxide layer, estimated based on the impedance data increases up to ~6 nm during 78 days of exposure. The observed fall in value of the $\log|Z|_{f=0.01\ \mathrm{Hz}}$ indicates a decrease in pitting corrosion resistance of Ti15Mo alloy in saline solution along with the immersion time. The detailed EIS study on the kinetics and mechanism of corrosion process and the capacitive behavior of the Ti15Mo electrode | passive layer | saline solution system was based on the concept of equivalent electrical circuit with respect to the physical meaning of the applied circuit elements. Potentiodynamic studies up to 9 V vs. SCE and SEM analysis show no presence of pitting corrosion what indicates that the Ti15Mo alloy is promising biomaterial to long-term medical applications.

Keywords: Biomaterial, corrosion resistance, passivation, structure, titanium alloys

1. Introduction

Titanium and its alloys are one of the most attractive materials utilized for both short- and long-term implants [1-5]. Those materials are characterized by good corrosion resistance in biological environment, relatively low toxicity of corrosion products and mechanical properties similar to the human bones. The corrosion products penetrating the surrounding tissue can be toxic, and thereby causing infection and necrosis [6]. Furthermore, pitting corrosion affects the fatigue strength of the implant leading to the mechanical damage [7]. That is why it is important to limit the corrosion of the implant in human body to a minimum. The most popular alloying elements for titanium alloys are aluminum which stabilizes α phase and vanadium the β stabilizer [8,9]. However those elements are harmful for human body and nowadays are replaced with inert elements e.g. Mo [1,2,4,5]. Moreover, the increase in the Mo content to 15% stabilizes the β phase and provides optimum mechanical and corrosion properties [4,5,10]. Due to the high oxygen affinity TiMo alloys are covered with stable, strongly adherent to the surface oxide layer which provides good corrosion resistance and protects material against the harmful influence of aggressive chloride ions present in human body [2,4,5,10]. In the literature, data on corrosion performance of the TiMo alloys in the biological environment for relatively short immersion time are available [2,4,5,10]. Therefore, the following work concerns the long-term corrosion resistance of the self-passive oxide layer present on the Ti15Mo alloy.

2. Experimental

Disc-shaped samples of the Ti15%wt. Mo alloy with a diameter of 10 mm were grounded with 80 to 2500# grit SiC paper and polished using final OP-S suspension. The crystal structure of the as-received Ti15Mo alloy was characterized by X-ray diffraction (XRD) and electron backscatter diffraction (EBSD) methods. For XRD method an X'Pert Philips PW 3040/60 diffractometer operating at 30 mA and 40 kV which was equipped with a vertical goniometer and an Eulerian cradle were used. The wavelength of radiation (λCuKα) was 1.54178Å. For measurements the Bragg-Brentano geometry was used. The EBSD measurements with step size 1.0 μm were performed on scanning electron microscope JEOL JSM-6480 equipped with a EBSD detector from Oxford Instruments. X-ray reflectometry (XRR) was used to determine the thickness of the oxide layer on the Ti15Mo before and after the electrochemical measurements. The XRR measurements were performed using a CuKα radiation on a PANalytical Empyrean

* UNIVERSITY OF SILESIA, INSTITUTE OF MATERIALS SCIENCE, 1A 75 PUŁKU PIECHOTY STR., 41-500 CHORZÓW, POLAND

Corresponding author: magdalena.szklarska@us.edu.pl

diffractometer equipped with PixCell^{3D} detector, five circle Eulerian cradle and multilayer X-ray mirror. The XRR data refinement were performed using GenX 2.4.9 analysis software based on the differential evolution algorithm assuming homogeneous layers with interface roughness [11]. Corrosion resistance was investigated in saline solution deaerated with argon (Ar, 99.999% purity) of pH = 7.4(1) at 37(2)°C. A three-electrode electrochemical cell was used. The Ti15Mo alloy was the working electrode. As a counter electrode the Pt mesh was used and the saturated calomel electrode (SCE) with a Luggin capillary was the reference electrode. The electrochemical measurements were carried out using a Metrohm/Eco Chemie Autloab PGSTAT30 Potentiostat/Galvanostat Electrochemical System. Prior to electrochemical measurements, the electrodes were depassivated at –1.2 V vs. SCE for 10 min. Open circuit potential (E_{OC}) was measured for 78 days. The electrochemical impedance spectroscopy (EIS) studies were performed at E_{OC} in the frequency range of 10 kHz-1 mHz. Ten frequencies per decade were scanned using a sine-wave amplitude of 10 mV. EIS data were analysed based on the concept of equivalent electrical circuits (EECs) using the EQUIVCRT program. Anodic polarization curves were registered potentiodynamically at a sweep rate $v = 4$ mV s^{-1} in the potential range from E_{OC} minus 150 mV to 9 V vs. SCE.

3. Results and discussion

XRD analysis confirmed that the Ti15Mo alloy is a solid solution of Mo in Ti matrix. On the diffraction pattern (Fig. 1) there are characteristic diffraction lines for β-titanium (ICDD PDF 01-089-4913) phase. The slight shift of the diffraction lines positions in comparison to the positions form the database is caused by the enlargement of the crystal unit cell. The addition of molybdenum atoms with larger atomic radii is the source of

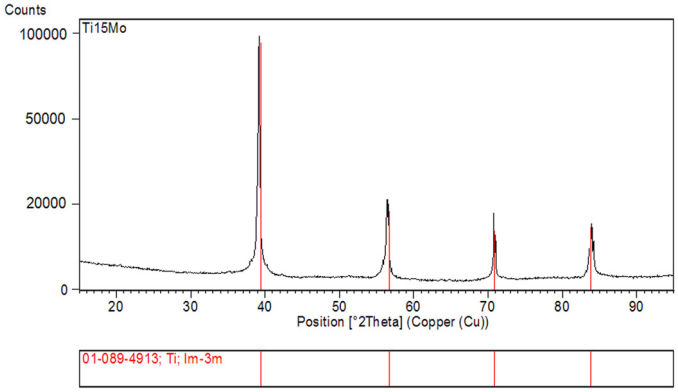

Fig. 1. XRD pattern of the as-received Ti15Mo alloy

lattice parameter increase. The SEM image and band contrast map of the as-received Ti15Mo alloy in Fig. 2 are consistent with the XRD results and confirm that in the Ti15Mo alloy only β-Ti phase with cubic structure (bcc) occurs. The XRR results (Fig. 3) show that self-passivated in air oxide layer present on as-received Ti15Mo alloy surface is 4.1(1) nm in thickness and its density is 3.9(1) g/cm^3. XRR study of the Ti15Mo electrode after 78 days of immersion in saline solution showed that the surface is covered with double-layer structured oxide (Fig. 3). The reliable fit to the experimental data could be achieved only by assuming two layers types. For each layers the thickness and density parameters were refined. The outer layer thickness was 2.1(2) nm and density was 1.65(3) g cm^{-3} indicating to porous structure. The inner-layer was more dense, 3.27(2) g cm^{-3}, with a thickness of 2.78(2) nm. These results confirm the bi-layer structure of the oxide film on the Ti15Mo electrode revealed in EIS measurements (Fig. 5).

During 78 days of exposure of the Ti15Mo electrode in saline solution at 37°C it could be observed that E_{OC} is strongly dependent on immersion time (Fig. 4). On the OCP curve (Fig. 4)

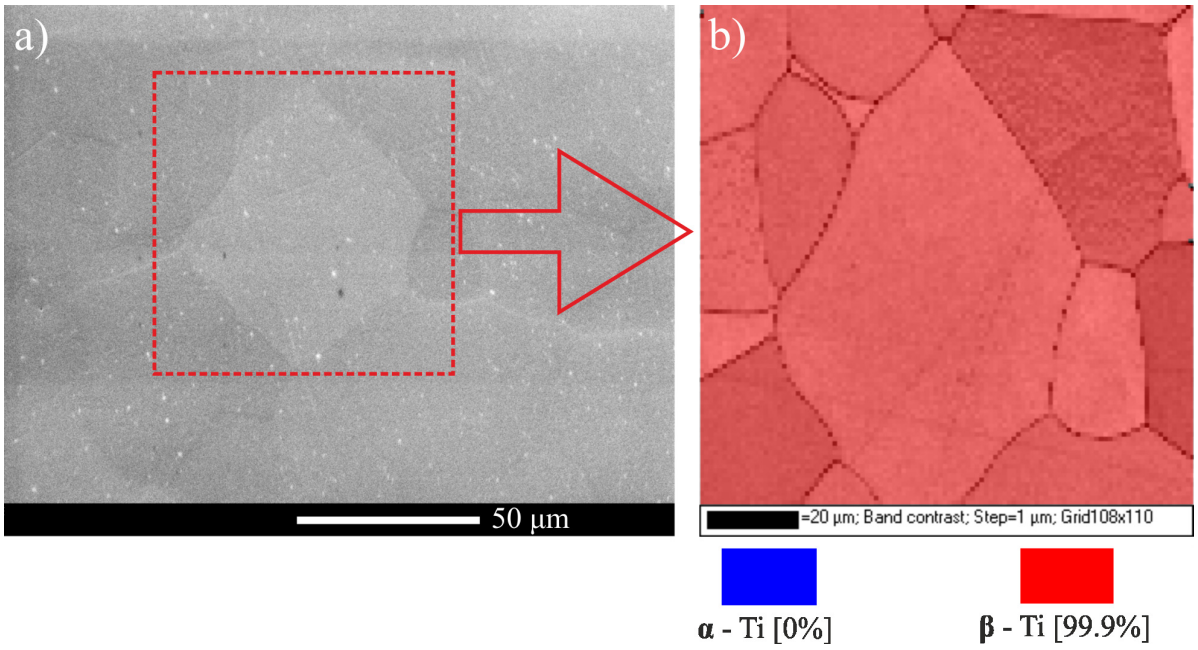

Fig. 2. SEM image a), band contrast map and phase map b) of the self-passivated Ti15Mo alloy

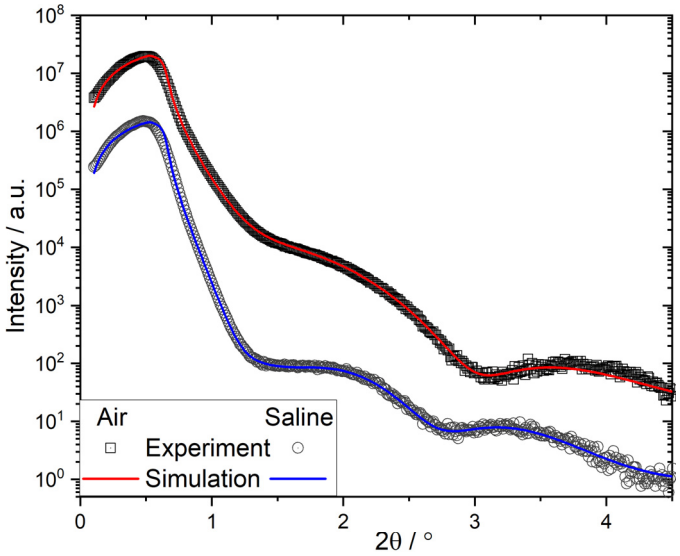

Fig. 3. X-ray reflectometry analysis of the Ti15Mo alloy: self-passivated in air and after exposure in saline solution at 37°C for 78 days

the rapid increase in potential right after immersion of the electrode could be observed. In the first two hours the ionic-electron equilibrium related to formation of double electrical layer at the electrolyte | passive layer interface was stabilized at the value of –0.3 V. In the next 5 days of immersion the potential gradually increased reaching –0.08 V. Then, up to 36 days E_{OC} oscillates around –0.1 V and after that slightly decreased until 56 days. It should be added that during that time a change of Ti oxide stoichiometry was possible and self-repair properties of Ti oxide layer plays an important role. After 56 days the potential was stabilized at –0.141 V and remained unchanged until the end of the long-term measurement indicating stability of the protective oxide layer. The thickness of the passive layer was determined as the function of the immersion time and it explains the increase of the OCP value.

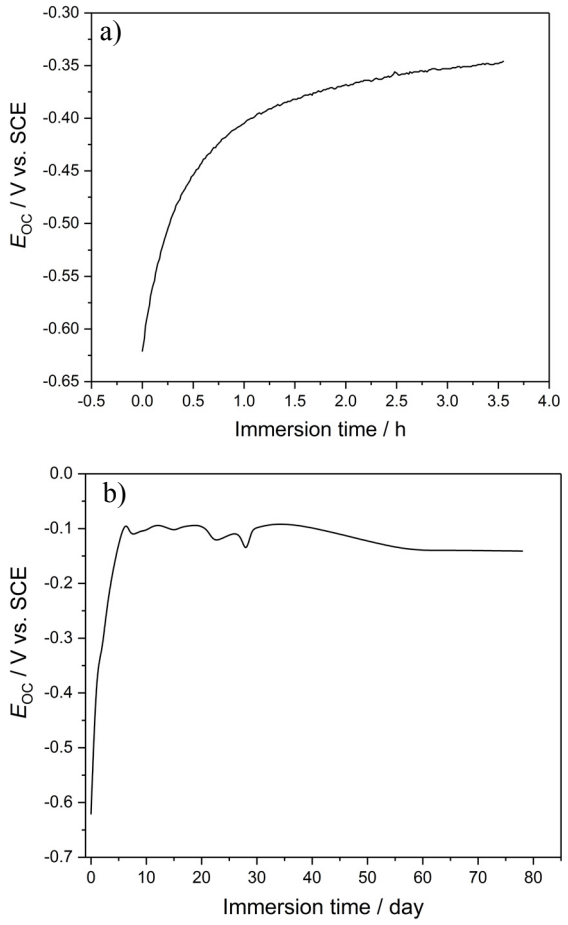

Fig. 4. Open circuit potential as a function of the immersion time for the Ti15Mo electrode in saline solution at 37°C for: 3.5 h a) and 78 days b)

The long-term corrosion resistance of the Ti15Mo |TiO_2| saline solution system was studied using EIS method. On experimental (symbol) Bode plots: $\log|Z| = f(\log f)$ and $-\varphi = f(\log f)$ (Fig. 5) one can observe the high values of $|Z|_{f\to 0}$ and φ close to −90° which are typical of a capacitive behavior of a high corrosion resistance material [3,12]. The higher impedance values (Fig. 5a) and the wider plateau (Fig. 5b) corresponding to the more effective corrosion resistance, were registered for the Ti15Mo electrode at the beginning of the test. With extension of the exposure time the two time constants at Bode-phase plot start to be clearly visible (Fig. 5b). It suggests that the oxide layer formed on the Ti15Mo electrode surface becomes porous with time and it is composed of a porous outer layer and dense inter layer which plays a role of the barrier layer against corrosion. A decrease in the $\log|Z|$ with time, especially in the low frequency range below 10 mHz, points the onset of pitting corrosion, however, the electrode still exhibits the properties of a corrosion-resistant material (Fig. 5a). The time constant at high frequencies arised from the uncompensated ohmic resistance related to the solution and the penetration of the solution through pores (pits) of the outer layer, and the time constant at low frequencies was associated with the processes at the barrier-type inner layer | solution interface. To analyze the pitting corrosion of the electrode covered with a bi-layered oxide film saline solution the suitable EEC model, presented in Fig. 6 was applied. This is a physical model representing the oxide layer formed on the Ti15Mo electrode surface which is composed of the porous outer layer and inner-barrier layer. In this model, the R_s element represents the resistance of the solution, R_p and C_p correspond to the resistance of solution in a pore (pit) and capacitance of the porous outer layer, respectively. C_b represents the capacitance and the R_b denotes the resistance of the inner-barrier oxide layer. In this model the capacitors were replaced with constant phase elements (CPE) representing a "leaking" capacitor, which has non-zero real and imaginary components. The CPE impedance is given by the following equation [1,2,12,13]:

$$\hat{Z}_{CPE} = \frac{1}{T(j\omega)^{\phi}} \tag{1}$$

where T is the capacitance parameter in $F\ cm^{-2}\ s^{\phi-1}$ which depends on the electrode potential, and ϕ is related to the angle of rotation of purely capacitive line on the complex plane plots: $\alpha = 90°(1 - \phi)$. Only when $\phi = 1$, $T = C_{dl}$ the purely capacitive behavior is obtained. Eqn. (1) represents pure capacitance for $\phi = 1$, infinite Warburg impedance for $\phi = 0.5$, pure resistance for $\phi = 0$, and pure inductance for $\phi = -1$.

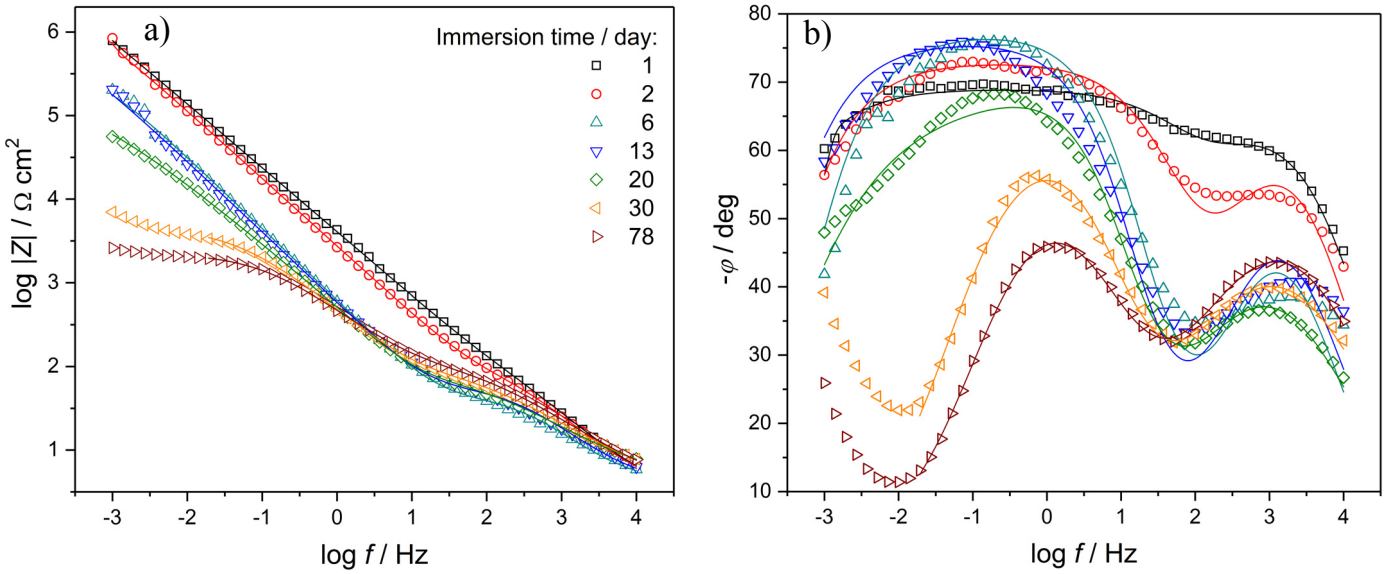

Fig. 5. Experimental (symbol) and approximated (line) Bode diagrams in the form of $\log|Z| = f(\log f)$ a) and $\varphi = f(\log f)$ b) for the Ti15Mo electrode in saline solution after different immersion time at 37°C

The results of the fitting procedure are presented in Table 1 and in the form of continuous lines in Fig. 5. The values of ϕ_p rapidly decrease in the first 20 days from 0.76(13) to 0.65(05) and then stabilize with tendency to slight increase until the end of experiment (Tab. 1). Those results indicate that with the immersion time the roughness and heterogeneities of the oxide layer change dynamically and the electrode surface become more porous. After 20 days the ϕ_p slightly increases what evidences that the oxide layer become more solid. These results are in good agreement with the values of capacitance characterized with T_p and resistance inside the pores. Rapid decrease in the R_p through the first three days from 375.2(144.1) to 117.5(2.5) Ω cm^2 corresponds with the increase of the surface porosity and indicates lowering in corrosion resistance of the outer porous oxide layer. Around 20th day of experiment the increase in the R_p was observed and evidenced for better protective properties of the outer oxide layer. The changes in T_p confirm weakening of corrosion resistance during first 20 days which is connected with increase of capacitance. With further time of experiment the T_p becomes lower what proves the improvement in corrosion resistance of the investigated electrode. The value of T_b parameter corresponding to capacitance of the barrier oxide layer increases with time

TABLE 1

The values of parameters obtained using the equivalent circuit model for pitting corrosion (see Fig. 6) to approximate experimental EIS data for the Ti15Mo electrode during long-term immersion in saline solution at 37°C; R_s = 4.1(0.3) Ω cm^2

Time day	Parameter					
	T_p/μF cm^{-2} s$^{\phi-1}$	ϕ_p	T_b/μF cm^{-2} s$^{\phi-1}$	ϕ_p	R_p/Ω cm^2	R_b/Ω cm^2
1	45.5(6.0)	0.763(0.013)	14.5(6.1)	0.779(0.044)	375.2(144.1)	5.5(0.8)×10^6
2	37.5(7.4)	0.792(0.020)	44.8(7.7)	0.827(0.021)	127.1(20.0)	2.2(0.3)×10^6
3	42.1(16.9)	0.837(0.045)	159.4(19.7)	0.943(0.024)	51.4(6.2)	1.2(0.3)×10^6
6	69.1(24.3)	0.780(0.039)	265.7(27.2)	0.880(0.020)	44.0(4.7)	3.6(0.5)×10^5
7	65.2(27.4)	0.791(0.047)	281.6(30.9)	0.885(0.021)	42.8(5.1)	6.0(1.3)×10^5
8	68.4(28.5)	0.784(0.047)	300.0(32.1)	0.878(0.021)	43.2(5.1)	6.2(1.5)×10^5
10	71.3(27.9)	0.774(0.044)	311.4(31.5)	0.870(0.020)	46.8(5.3)	5.8(1.3)×10^5
13	69.8(20.7)	0.762(0.033)	296.9(23.5)	0.866(0.016)	57.3(5.2)	7.5(1.8)×10^5
16	101.1(20.6)	0.730(0.023)	332.0(22.4)	0.838(0.013)	54.6(3.8)	3.0(0.5)×10^5
17	132.9(15.9)	0.691(0.013)	328.9(17.5)	0.827(0.011)	60.2(3.1)	1.5(0.1)×10^5
20	236.8(8.3)	0.625(0.004)	259.8(9.9)	0.859(0.010)	81.6(2.7)	1.7(0.1)×10^5
21	247.8(10.1)	0.618(0.004)	256.3(11.1)	0.857(0.010)	85.0(2.9)	9.5(0.7)×10^4
23	227.8(20.9)	0.622(0.010)	277.1(19.7)	0.839(0.015)	90.9(4.9)	5.1(0.1)×10^3
26	204.8(17.4)	0.631(0.010)	301.6(16.4)	0.824(0.011)	95.0(4.3)	4.9(0.1)×10^3
30	217.5(17.2)	0.617(0.009)	330.5(16.5)	0.798(0.010)	104.3(4.6)	4.5(0.1)×10^3
37	211.5(13.8)	0.618(0.007)	367.4(13.7)	0.761(0.007)	107.0(4.0)	4.3(0.1)×10^3
57	179.5(9.8)	0.632(0.006)	440.7(10.3)	0.716(0.005)	102.4(3.0)	4.0(0.1)×10^3
78	143.2(6.0)	0.651(0.005)	447.9(6.9)	0.718(0.004)	117.5(2.5)	2.2(0.1)×10^3

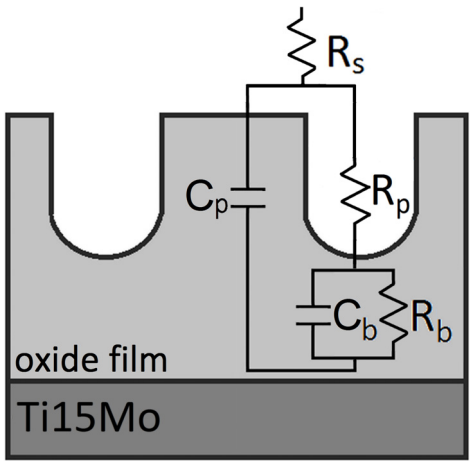

Fig. 6 Equivalent electrical circuit for the pitting corrosion of the Ti15Mo electrode covered with a bi-layered oxide film in saline solution

which indicat that the exposed surface area of the electrode increases due to uncovering of pinholes. The highest value of R_b 5.5(8)·10^6 Ω cm^2 points to the strongest protective properties of the barrier oxide layer at the first day of immersion. The R_b parameter rapidly decreases to 3.6(5)·10^5 Ω cm^2 during first six days. With further exposition the R_b slowly getting lower and after 23 day stabilizes around 5.1(1)·10^3 Ω cm^2. The ϕ_b values changes slightly from 0.78(4) at the beginning of the test to 0.72(04) at the end of exposure confirming the relative stability of the inner-barrier layer.

The average values of capacitance of an electrical double layer, $\bar{C}_{dl}$ for the formed oxide layer | saline solution system were determined from the formula given by Brug et al. [13].

$$T_{dl} = \bar{C}_{dl}^{\phi_{dl}} (R_s^{-1} + R_{ct}^{-1})^{1-\phi_{dl}} \quad (2)$$

The rapid growth of the C_{dl} value with the first three days of the experiment suggest to weakening of the tested alloy corrosion resistance (Fig. 7). Within further study the corrosion resistance is improved what can be concluded based on the dynamical decrease of the C_{dl} up to 21st day when it stabilizes at 3.8(2) μF cm^{-2} and remains almost unchanged to the last day of exposure. Influence of immersion time on the pitting corrosion resistance of the tested electrode was evaluated by the value of log |Z| at the lowest frequency studied of f = 1 mHz (Fig. 8). On the first day the value of log $|Z|_{f=1\ \mathrm{mHz}}$ was high and equaled to 6.2(3) Ω·cm^2. Through 21 days the value of log $|Z|_{f=1\ \mathrm{mHz}}$ dynamically decreased to 3.8(2) Ω cm^2 and then was stabilized reaching the value of 3.4(2) Ω cm^2 in 78 days. This result indicates the increasing susceptibility to pitting corrosion of the Ti15Mo electrode with time of immersion in saline solution due to the presence of chloride ions responsible for pitting attack [2,4,5,10].

The thickness of the oxide layer (d_{ox}) formed on the Ti15Mo electrode surface during long-term corrosion study was estimated based on the experimental EIS data and the formula proposed by Birch and Burleigh [14]:

$$d = \varepsilon_0 \varepsilon 2\pi S f (Z - Z_0) \quad (3)$$

where: f – the frequency at which the phase angle (φ) reaches a maximum, Z – impedance at the frequency f, Z_0 – impedance at high frequencies (electrolyte resistance), S – area of the tested surface, ε_0 – dielectric constant for free space (8.854·10^{-12} F/m), ε – dielectric constant for TiO_2 (114) [15] and MoO_3 (16) [16].

On the first day it was rapid, tenfold growth of the d_{ox} reaching 5.8(3) nm in thickness (Fig. 8). In the next day the oxide layer was slightly dissolved and the thickness was lower to be 4.7(2) nm, and then slowly growed and stabilized reaching the value of 6.4(3) nm in 78 days. These results correspond with the changes in the values of log $|Z|_{f=1\ \mathrm{mHz}}$. The growing oxide layer become porous which causes a decrease in value of log $|Z|_{f=1\ \mathrm{mHz}}$. Lowering of this value is observe because the solution accumulates in the pores, the local pH is changed and the corrosive nanocells are formed which promotes faster dissolution of the material inside the pores.

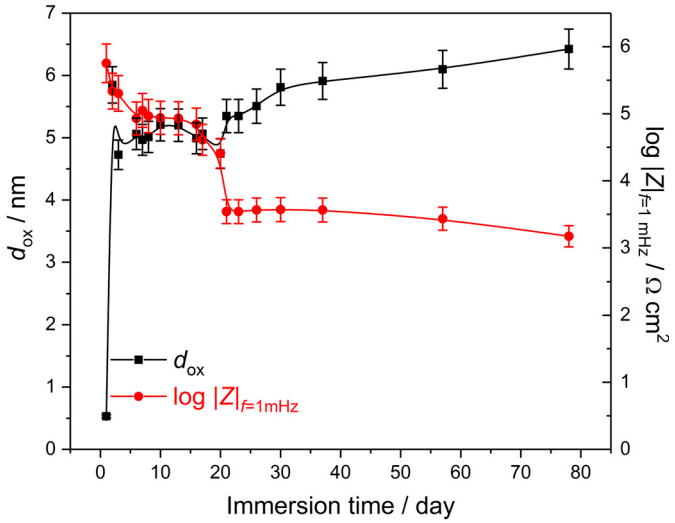

Fig. 7. The double layer capacitance as a function of the immersion time for the Ti15Mo electrode in saline solution at 37°C

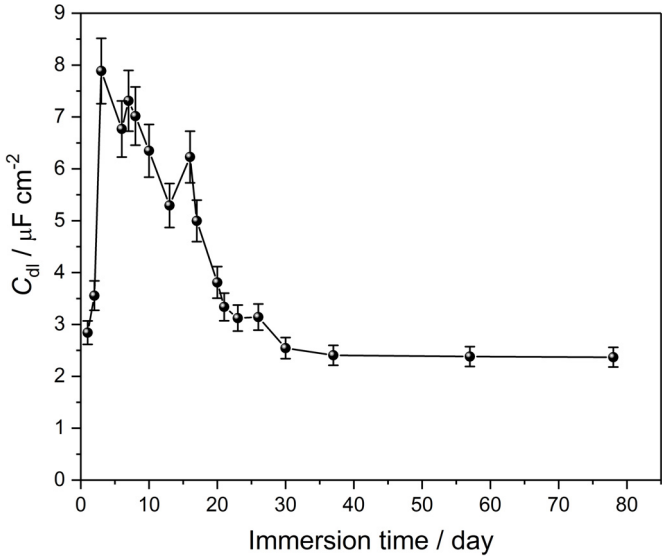

Fig. 8. The experimental values of log |Z| at f = 0.001 Hz (○), and calculated based on impedance data thickness of the inner-barrier oxide layer (□) for various immersion time of the Ti15Mo electrode in saline solution at 37°C

The registered potentiodynamic curves is typical for self-passivating material. The lack of a rapid increase in the value of current densities indicates that the oxide layer present on the surface of the tested alloy did not break through to the potential value of 9 V vs. SEC and still providing protective function (Fig. 9). After 78 days, the porous oxide layer formed on the Ti15Mo surface could be composed of nonstoichiometric oxides of titanium and molybdenum. On the potentiodynamic curve registered for the Ti15Mo electrode after 78 days of exposure in saline solution the increasing in current density around 2 V could be observed. Also the passive (2,5-4 V vs. SEC) and transpassive (7-9 V vs. SEC) range can be distinguished. This result might be connected with the oxidation of the nonstoichiometric oxides during increasing of potential value.

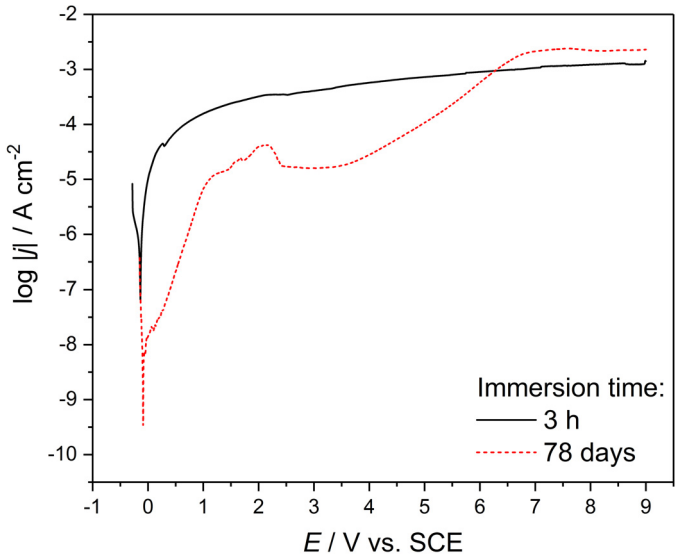

Fig. 9. Anodic polarization curves (v = 4 mV s^{-1}) for the Ti15Mo electrode after 3 h and 78 days of immersion in saline solution at 37°C

It seems that Mo as an alloying addition stabilizes the passive layer against breakdown and pit initiation could be slowed down or primary suppressed. Comparison of these results with the breakdown potential of 1-2 V for TiO_2 oxide layer on pure Ti and its alloys in a biological milieu [2,3] indicates the possibility of application of the Ti15Mo in medicine. Also the SEM analysis of the Ti15Mo alloy surfaces after corrosion tests have not revealed the presence of pitting corrosion.

4. Conclusions

The β-type Ti15Mo alloy has a good corrosion resistance in saline solution due to ability to spontaneous passivation. Long-term study of the Ti15Mo electrode corrosion resistance shows that its resistance to pitting corrosion decreases with time. The potentiodynamic studies up to 9 V vs. SCE and SEM analysis show no presence of pitting corrosion. The bi-layer character of the formed oxide layer during immersion of the Ti15Mo electrode in saline solution was confirmed by EIS data and XRR analysis. The corrosion parameters calculated through approximation of EIS data evidence that corrosion resistance of investigated material dynamically changed during the first 20 days. Through the first 3 days the strong lowering of corrosion resistance was observed. Till then the corrosion properties were improved and started stabilized after 20th day of immersion. The time of immersion has significant influence on the oxide layer thickness which changed from 0.5(3) nm in first day of immersion to 6.4(3) nm on 78 day of test. As the thickness and porosity of the oxide layer was growing the value of log $|Z|_{f=1\ mHz}$ was decreasing. Performed research show that the Ti15Mo alloy meets the criteria of corrosion resistance for biomaterials to long-term medical applications.

Acknowledgments

Financial support from BS 1S-0816-001-1-10-01 (Poland) is acknowledged.

REFERENCES

[1] M. Szklarska, G. Dercz, W. Simka, B. Łosiewicz, Surf. Interface Anal. **46**, 698-701(2014).
[2] M. Szklarska, G. Dercz, J. Rak, W. Simka, B. Łosiewicz, Arch. Metall. Mater. **60**, 2687-2694 (2015).
[3] M. Freitag, B. Łosiewicz, T. Goryczka, J. Lelątko, Solid State Phenom. **183**, 57-64 (2012).
[4] N.T.C. Oliveira, G. Aleixo, R. Caram, A.C. Guastaldi, Mater. Sci. Eng. A **452-453**, 727-731 (2007).
[5] W. Simka, A. Krząkała, D.M. Korotin, I.S. Zhidkov, E.Z. Kurmaev, S.O. Cholakh, K. Kuna, G. Dercz, J. Michalska, K. Suchanek, T. Gorewoda, Electrochim. Acta **96**, 180-190 (2013).
[6] C.C. Shih, S.J. Lin, Y.L. Chen, Y.Y. Su, S.T. Lai, G.J. Wu, C.F. Kwok, K.H. Chung, J. Biomed. Mater. Res. **52**, 395-403 (2000).
[7] M. Geetha, U. Kamachi Mudali, A.K. Gogia, R. Asokamani, R. Baldev, Corros. Sci. **46**, 877-892 (2004).
[8] D.J. Maykuth, F.C. Holden, D.N. Williams, H.R. Ogden, R.I. Jaffee, The effects of alloying elements in titanium, Defense metals information center, Ohio (1961)
[9] I. Halevy, G. Zamir, M. Winterrose, G. Sanjit, Carlos Roberto Grandini, Ariel Moreno-Gobbi, J. Phys.: Conf. Ser. **215**, 012013 (2010).
[10] N.T.C. Oliveira, A.C. Guastaldi, Acta Biomater. **5**, 399-405 (2009).
[11] M. Björck, G. Andersson, GenX: an extensible X-ray reflectivity refinement program utilizing differential evolution, J. Appl. Cryst. **40**, 1174-1178 (2007).
[12] A. Lasia, Electrochemical impedance spectroscopy and its applications. Springer Science+Business Media, New York (2014).
[13] G.J. Brug, A.L.G. van den Eeden, M. Sluyters-Rehbach, J.H. Sluyters, J. Electroanal. Chem. **176**, 275-295 (1984).
[14] J.R. Birch, T.D. Burleigh, Corros. **56**, 1233-1241 (2000).
[15] R.A. Parker, Phys. Rev. **124**, 1719-1722 (1961).
[16] G.S. Nadkarni, J.G. Simmons, J. Appl. Phys. **41**, 545-551 (1970).